

# Analytical solitary wave solutions of the nonlinear Kronig-Penney model in photonic structures

Y. Kominis

School of Electrical and Computer Engineering, National Technical University of Athens, Zographou GR-15773, Greece

(Received 6 December 2005; revised manuscript received 16 May 2006; published 19 June 2006; corrected 7 July 2006)

A phase space method is employed for the construction of analytical solitary wave solutions of the nonlinear Kronig-Penney model in a photonic structure. This class of solutions is obtained under quite generic conditions, while the method is applicable to a large variety of systems. The location of the solutions on the spectral band gap structure as well as on the low dimensional space of system's conserved quantities is studied, and robust solitary wave propagation is shown.

DOI: [10.1103/PhysRevE.73.066619](https://doi.org/10.1103/PhysRevE.73.066619)

PACS number(s): 42.70.Qs, 42.65.Tg, 42.65.Wi, 42.82.Et

## I. INTRODUCTION

The study of spatially localized modes in periodic optical structures, consisting of arrays of nonlinear optical waveguides, is a field of continuously increasing research interest from both the experimental and the theoretical point of view [1–3]. In contrast to the case of homogeneous structures, where the corresponding models can be integrable and soliton propagation occurs, periodically inhomogeneous systems are typically nonintegrable. This fact excludes the possibility of pure soliton existence (in the strict mathematical sense, this prerequisites complete integrability), but also gives rise to the potentiality of existence of a plethora of solitary waves which do not have a counterpart in the homogeneous cases. Although, these structures are not solitons, they can exhibit a quite robust behavior under propagation, a property that considerably facilitates their experimental observation [4–6].

From the theoretical point of view, in order to study these structures, a variety of models and different approaches has been considered, including: the tight-binding approximation, based on the assumption of weakly coupled waveguides and leading to a discrete nonlinear Schrödinger equation (D-NLSE) [7], and the coupled-mode theory, based on the assumption of strong coupling and resulting to a set of coupled equations governing the forward and backward wave propagation [8]. On the basis of these approaches, the existence of various solitary wave modes has been shown and their propagation has been studied [3]. However, both methods are strongly restricted to specific limits of the configuration parameter range [1,9]. In order to overcome these restrictions and study the solitary wave formation in a unified model, the original NLSE, with periodically varying coefficients, modeling the waveguide array structure, has to be considered

$$i \frac{\partial \psi}{\partial z} + \frac{\partial^2 \psi}{\partial x^2} + \epsilon(x) \psi + g(x, |\psi|^2) \psi = 0, \quad (1)$$

where  $z$ ,  $x$ , and  $\psi$  are the normalized propagation distance, transverse dimension, and electric field, respectively. The periodic transverse variation of the linear refractive index is given by  $\epsilon(x)$ , while the spatial and intensity dependence of the nonlinear refractive index is provided through  $g(x, |\psi|^2)$ . This improved model has been studied in the special cases where the periodic transverse inhomogeneity is restricted either to the linear [10–12] or the nonlinear refractive index

[13], while the transverse profile of the inhomogeneity has been assumed to have the form of the so-called Dirac comb. The nonperiodic case of the presence of a single delta-shaped nonlinear defect in a medium with periodic linear refractive index has also been studied [14]. Within this approach the linear band structure of the model has been shown and localized modes with various symmetries have been provided. However, it is obvious that a Dirac comb description of the spatial dependence of the nonlinearity can render only qualitative results and is far from being generic and adequate for describing realistic configurations.

## II. MODEL AND ANALYTICAL SOLUTIONS

In this work, we consider the case of a realistic model described by (1) with piecewise-constant coefficients [15], namely a nonlinear Kronig-Penney type of model. This model is more general than the aforementioned ones, which are contained as limiting cases of the model in hand. Moreover, we describe an exact method, based on phase space analysis, which can be used in order to obtain, analytically, generic classes of stationary solutions of the model, having the form of solitary waves. Such phase space methods have been applied so far only in cases with localized (nonperiodic) transverse inhomogeneity [16–18]. In the following we show that the analytically obtained stationary solutions are localized modes which include both symmetric and asymmetric wave profiles, while their propagation shows a remarkable robustness, which is promising for photonic applications.

The stationary solutions of (1) have the form  $\psi(x, z) = u(x; \beta) e^{i\beta z}$ , and satisfy the nonlinear ordinary differential equation

$$\frac{d^2 u}{dx^2} + [\epsilon(x) - \beta] u + g(x, u^2) u = 0, \quad (2)$$

where  $\beta$  is the propagation constant and  $u(x; \beta)$  is the real transverse wave profile. Equation (2) describes a nonautonomous nonlinear dynamical system which is in general nonintegrable. The complexity of the dynamical system is evident, even in the limiting case where the transverse variation of the linear and nonlinear refractive index is considered as a small perturbation to an autonomous system with constant coefficients, corresponding to the mean values of  $\epsilon(x)$  and  $g(x, u^2)$ . When the unperturbed system has a homoclinic orbit, which is the case of interest for the solitary wave forma-

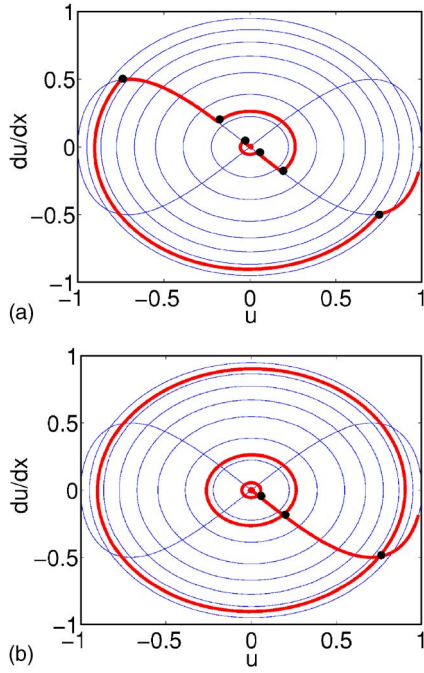


FIG. 1. (Color online) Phase space construction of asymptotic (solitary) solutions of (2) for  $n$ , odd (a), and  $n$ , even (b). Black dots depict transition at the boundary between a linear and a nonlinear layer.

tion, Melnikov’s theorem [19] predicts the formation of a homoclinic tangle and the presence of homoclinic chaos, resulting in a complex transverse profile for the stationary solitary wave.

We consider the case of a periodic structure consisting of linear and nonlinear layers, with the linear and the nonlinear refractive index given by

$$[\epsilon(x), g(x, u^2)] = \begin{cases} [\epsilon_n, N(u^2)], & x \in U_N \\ (\epsilon_l, 0), & x \in U_L \end{cases}, \quad (3)$$

where  $U_N = \cup_k (kT - N/2, kT + N/2)$ ,  $U_L = \cup_k [kT + N/2, (k + 1)T - N/2]$ ,  $N(u^2)$  is the nonlinearity function,  $L$  and  $N$  are the lengths of the linear and the nonlinear layers, respectively, and  $T = L + N$  is the spatial period of the structure. In each part of the photonic structure the wave profile is described from the following equations:

$$\frac{d^2u}{dx^2} + (\epsilon_n - \beta)u + N(u^2)u = 0, \quad x \in U_N, \quad (4)$$

$$\frac{d^2u}{dx^2} + (\epsilon_l - \beta)u = 0, \quad x \in U_L. \quad (5)$$

The stationary solutions of (2) can be provided by composing solutions of these two systems, which have matched conditions for  $u$  and its derivative, at the interfaces. Furthermore, we assume that the propagation constant  $\beta$  is such that: (1) the linear system has periodic (sinusoidal) solutions, and (2) the nonlinear system has a homoclinic orbit, tending

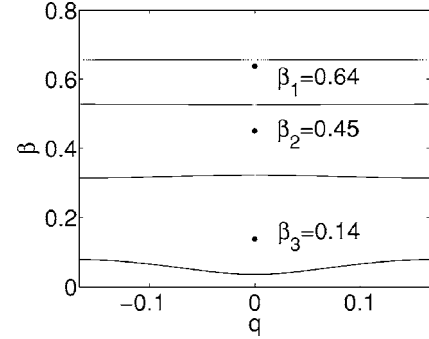


FIG. 2. Band structure of the linearized system (propagation constant  $\beta$  vs Bloch wave number  $q$ ) for a photonic structure having  $L = 4\pi$ ,  $N = 2\pi$ ,  $\epsilon_n = 0$ , and  $\Delta\epsilon = 0.7$ . Black dots depict the location of the analytically obtained localized modes for  $n = 1, 2, 3$ .

to the origin for  $x \rightarrow \pm\infty$  and being symmetric with respect to the origin. For a propagation constant corresponding to the case where an integer number of half periods of the solution of the linear system is contained in the linear part of length  $L$ , i.e.,

$$\beta_n = \epsilon_l - \left(\frac{n\pi}{L}\right)^2, \quad n = 1, 2, \dots, \quad (6)$$

the continuity conditions are met simultaneously in all boundaries: any solution of (2) starting from a point of the homoclinic orbit inside the nonlinear part at some  $x$  returns to the homoclinic orbit after evolving in the linear part and subsequently evolves again according to the homoclinic orbit. Thus, the solution approaches the origin asymptotically as  $x \rightarrow +\infty$ , moving on the homoclinic orbit but interrupted periodically due to the linear part of the structure. The same argument holds for the evolution of the stationary solution as  $x \rightarrow -\infty$ . These arguments are illustrated in Fig. 1, where the phase space representation of the homoclinic orbit and the phase space of the linear system have been superimposed. The branches of solutions are shown to coincide with parts of the (nonlinear) homoclinic orbit and parts of the (linear) periodic ellipsoid orbits. Several properties and symmetries of the solutions can be derived from their phase space representation: for odd  $n$  [Fig. 1(a)], the solutions lie in both branches of the homoclinic orbit so that  $u$  has an alternating sign between neighboring nonlinear layers, while modes with constant sign of  $u$ , lying exclusively in one branch, are obtained for even  $n$  [Fig. 1(b)]. Following the same arguments, not only asymptotic (solitary) solutions, but also nonlinear periodic stationary solutions can be generated. In fact, for  $\beta = \beta_n$  the entire Poincare surface of section (including both asymptotic and periodic orbits) of the system (2) as defined stroboscopically (with respect to  $x$ ) is identical to the phase space of the nonlinear system, while for  $\beta \neq \beta_n$  the Poincare surface of section appears chaotic. This abrupt change of the phase space topology for the specific values of  $\beta$ , has a form of a *global bifurcation*. More specifically, for the asymptotic solutions,  $\beta_n$  are values for which a complete homoclinic tangency occurs, resulting in an infinite set of

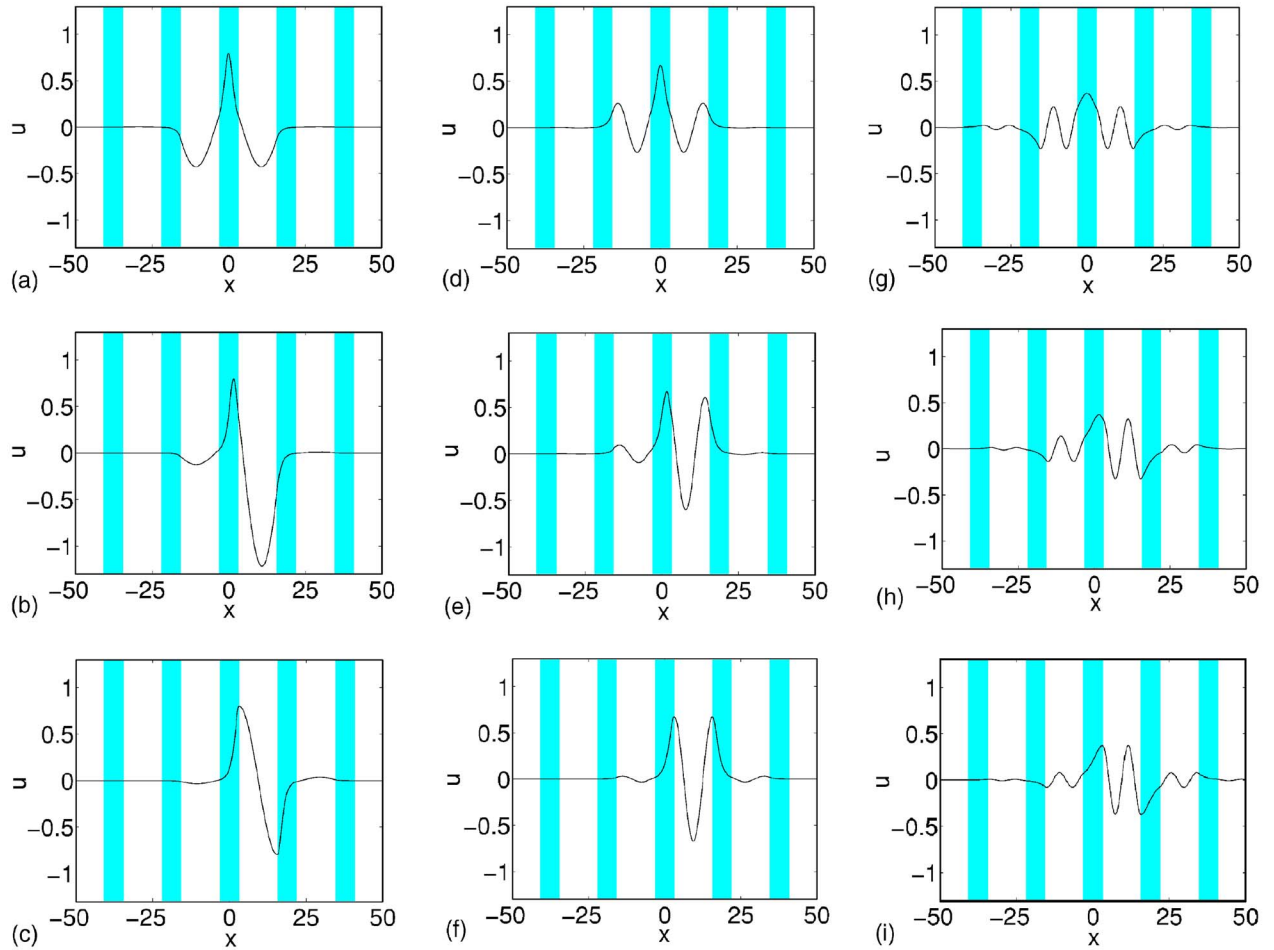


FIG. 3. (Color online) Analytically obtained profiles of solitary wave solutions, for  $n=1, 2, 3$  (left to right). Shaded areas correspond to nonlinear layers. The first and third row depict solutions having a symmetry with respect to the center of the linear ( $x_0=0$ ) and the nonlinear ( $x_0=N/2$ ) layer, respectively. The middle row depicts asymmetric solutions ( $x_0=N/4$ ). All parameters are the same as in Fig. 2.

solutions, each one starting from a different point of the homoclinic orbit; for  $\beta \neq \beta_n$  it is expected that the stable and unstable manifolds intersect transversely [19] and only some of these solutions, corresponding to intersection points, persist.

The solitary wave stationary solutions corresponding to  $\beta_n$  can be given analytically in the following form:

$$u(x; \beta_n, x_0) = \begin{cases} (-1)^{nk} v(x - kL; \beta_n, x_0) & x \in U_N \\ a_k \sin(\sqrt{\epsilon_l - \beta_n} x + \phi_k) & x \in U_L \end{cases}, \quad (7)$$

where  $v(x; \beta, x_0)$  is the homoclinic solution of the nonlinear system (4) and  $(a_k, \phi_k)$  are directly obtained from the continuity conditions of  $u$  and its derivative at the interfaces. The homoclinic solution, in general, is given by

$$x - x_0 = \pm \int_{v_m}^v \frac{dv'}{\sqrt{(\beta - \epsilon_n)v'^2 - F(v')}} \quad (8)$$

with  $F$  being defined by  $dF/du = 2N(u^2)u$ , and  $v_m$  is the non-zero root of the denominator in the integrand, corresponding to the extreme value of the solution, which is placed at  $x_0$ .

### III. RESULTS AND DISCUSSION

Although the method, presented in the previous section, applies in a general class of nonlinearities, for illustrative purposes, in the following we consider the case of a Kerr-type self-focusing nonlinearity,  $N(u^2) = 2u^2$ . In this case, the second assumption of the existence of a homoclinic orbit results in the condition

$$\beta_n > \epsilon_n \quad (9)$$

and the homoclinic solution is  $v(x; \beta, x_0) = \pm \sqrt{\beta - \epsilon_n} \operatorname{sech}[\sqrt{\beta - \epsilon_n}(x - x_0)]$ . As it can be seen from (6) and (9) the conditions for existence of the aforementioned solutions are quite generic: *solutions of the form (7) exist for a positive linear refractive index difference  $\Delta\epsilon \equiv \epsilon_l - \epsilon_n$ , and for discrete values of the propagation constant.*

In general, the geometry of the structure is crucial for both the existence and the form of the localized modes. The number of modes for a given  $\Delta\epsilon$  depends on the length ( $L$ ) of the linear part of the periodic structure: *for increasing  $L$ , the number and the density of the modes  $\beta_n \in (\epsilon_n, \epsilon_l)$ , also increase.* Each value  $\beta_n$  is located inside a finite band gap, of the spectral band structure of the linearized system associ-

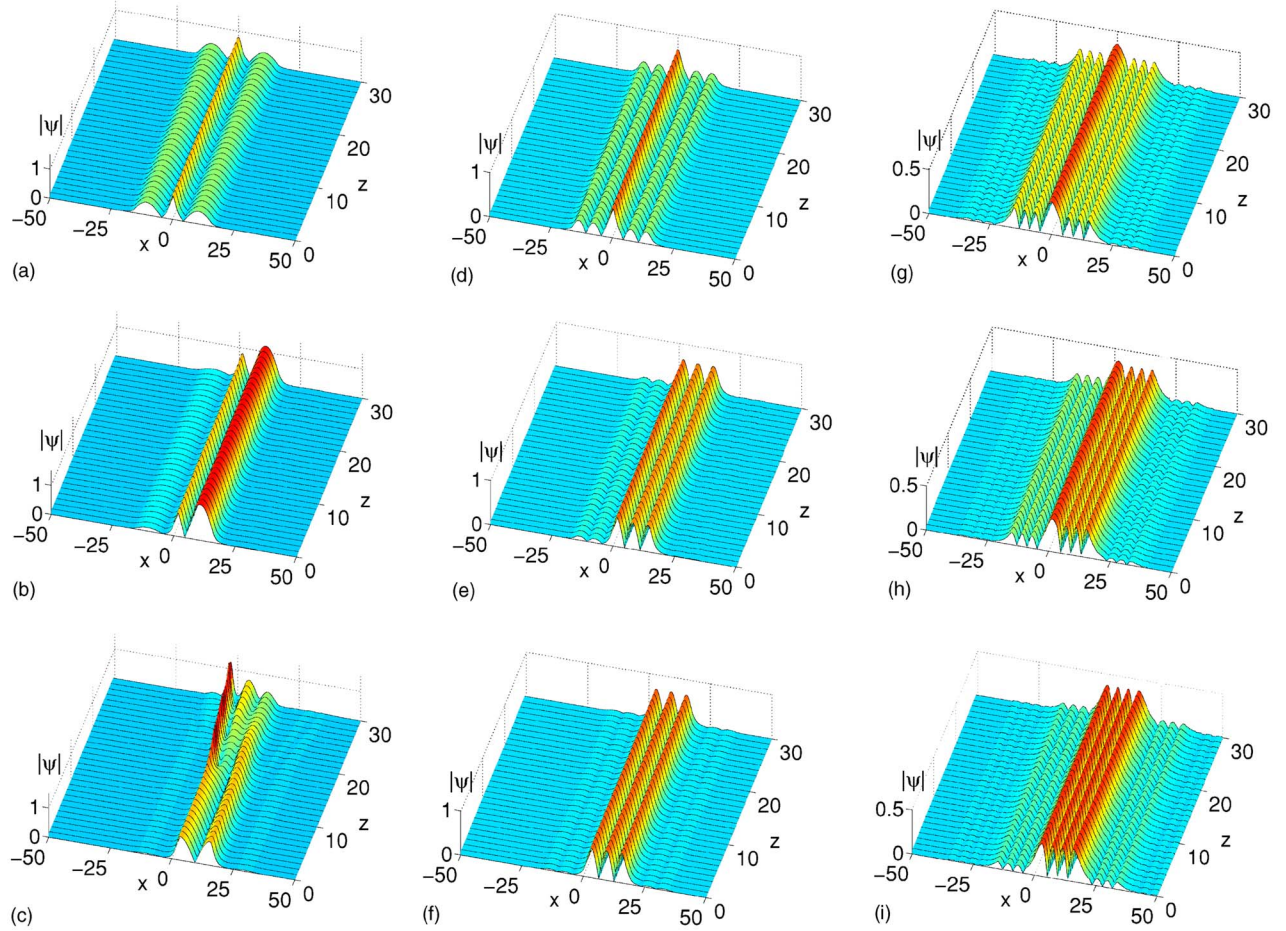


FIG. 4. (Color online) Propagation of solitary wave solutions for a photonic structure having the same parameters as in Fig. 2. The solutions correspond to  $n=1, 2, 3$  (left to right) and  $x_0=0, N/4, N/2$  (top to bottom).

ated to (1), which corresponds to a resonant Bragg-type reflection from the periodic structure [20]. On the other hand, the length  $N$  of the nonlinear layer determines the spatial width of the solution, since for large  $N$  the solutions are strongly localized in the nonlinear layer, and only small side-lobes appear in the neighboring linear layers.

As an example, we consider the case of a linear refractive index difference  $\Delta\epsilon=0.7$ , where we have set  $\epsilon_n=0$ , without loss of generality, since a nonzero  $\epsilon_n$  results only in a shift in the values of  $\beta_n$ , as obtained from (6) and (9). The length of the linear and nonlinear layers are  $L=4\pi$  and  $N=2\pi$ , respectively. According to the existence conditions (6) and (9), for this parameter set, three families of solutions, corresponding to  $n=1, 2, 3$ , are found. The location of  $\beta_n$  in the band structure of the linear system is illustrated in Fig. 2, where it is shown that each  $\beta_n$  is representative for a finite gap. Each family of localized solutions, corresponding to  $\beta_n$ , is parameterized by the location of the maximum of the homoclinic part of the solution in the nonlinear layer,  $x_0 \in [-N/2, N/2]$ . Due to symmetry of the structure with respect to  $x=0$ , we can restrict our analysis to solutions with  $x_0 \in [0, N/2]$ . In Fig. 3, we show the profiles of several stationary localized solutions, corresponding to  $n=1, 2, 3$  and  $x_0=0, N/4, N/2$ . The mode number  $n$ , determines the number of nodes of the

solution in the linear parts of the structure, as well as the constancy ( $u$ , even) or the alternation ( $u$ , odd) of the sign of  $u$  in the nonlinear parts. On the other hand,  $x_0$  determines the symmetry of the solutions. Thus, for  $x_0=0$ , we have modes which are symmetric with respect to the center of the nonlinear layer (Fig. 3, top row), while for  $x_0=N/2$ , the modes can be either symmetric ( $n$ , even) or antisymmetric ( $n$ , odd), with respect to the center of the linear layer (Fig. 3, bottom row). For  $x_0 \neq 0, N/2$ , we can have a general class of asymmetric localized modes (Fig. 3, middle row).

The evolution of several characteristic localized modes, obtained analytically with the aforementioned method, is depicted in Fig. 4. The propagation has been simulated using the standard beam propagation method for the numerical solution of Eq. (1). In all numerical simulations, a random noise of the order of  $10^{-2}$  (with respect to the maximum of the stationary solution) has been superimposed to the solution. The normalized propagation distance  $z_{max}=30$  corresponds to an actual propagation length of 3.2–7.3 mm, for the case of a nonlinear material of AlGaAs type, when the transverse coordinate is normalized to  $X_0=2-3 \mu\text{m}$ . It is shown that modes corresponding to  $n=2, 3$  are quite robust under propagation, while for  $n=1$  the mode corresponding to  $x_0=N/2$ , is unstable. This kind of instability is typical for gap solitons in lattices and periodic media [14, 21–23] and

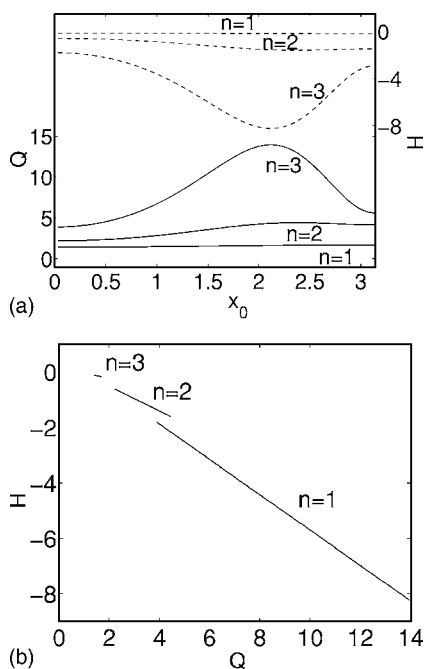


FIG. 5. (a) Energy  $Q$  (solid lines) and Hamiltonian  $H$  (dashed lines) vs  $x_0$ . (b) Hamiltonian vs energy diagram. All parameters are the same as in Fig. 2.

occurs when  $\beta$  is large enough so that an internal (discrete) mode [24] of the linear spectrum of the solution crosses into a linear transmission band (shown in Fig. 2) and resonates with the linear Bloch waves. Such instabilities can trigger various types of spatial dynamics including the symmetry breaking and oscillatory instabilities [14,21–23], as well as mode transformation scenarios according to which an unstable localized mode evolves (transforms) to a stable one [25]. However, it is worth mentioning that in experimental configurations, even if some kind of instability occurs, the laminar propagation distance in several cases is much larger

than the actual length of the device (as for the aforementioned case of an AlGaAs type of nonlinear material). This fact is quite promising for potential applications.

Finally, it is useful to locate the analytically obtained solutions in the low dimensional space of specific conserved quantities. The Hamiltonian  $H$  and energy  $Q$  functionals are calculated for each family of solutions as shown in Fig. 5(a). The representation (projection) of the families of solutions in the Hamiltonian-Energy plane is depicted in Fig. 5(b), and can be used for providing an overview of the analytically obtained solutions. It is shown that, solutions having the same  $\beta_n$  and different  $x_0$  lie on the same straight line with slope  $dH/dQ = -\beta_n$ , in accordance with Refs. [25,26].

#### IV. CONCLUSIONS

In conclusion, in this work we have used a phase space analysis method in order to derive analytically a generic class of localized stationary solutions for the nonlinear Kronig-Penney model, governing beam propagation in a photonic structure. These solutions correspond to symmetric or asymmetric solitary wave solutions which are shown to exhibit quite robust behavior under propagation. Moreover, the phase space method presented suggests a general approach for providing solitary or nonlinear periodic wave solutions, with potential applicability to a wide range of nonlinear models of wave propagation in structured media.

#### ACKNOWLEDGMENTS

The author would like to thank Professor K. Hizanidis for valuable guidance and comments on this work, and Dr. N. K. Efremidis for stimulating discussions on nonlinear photonic structures. The project is cofunded by the European Social Fund (75%) and National Resources (25%)-Operational Program for Educational and Vocational Training II (EPAEK II) and particularly the Program PYTHAGORAS.

- [1] A. A. Sukhorukov, Y. S. Kivshar, H. S. Eisenberg, and Y. Silberberg, *IEEE J. Quantum Electron.* **39**, 31 (2003).
- [2] J. W. Fleischer, G. Bartal, O. Cohen, T. Schwartz, O. Manela, B. Freedman, M. Segev, H. Buljan, and N. K. Efremidis, *Opt. Express* **13**, 1780 (2005).
- [3] *Discrete Solitons*, edited by S. Trillo and W. Torruellas (Springer-Verlag, Berlin, 2001).
- [4] H. S. Eisenberg, Y. Silberberg, R. Morandotti, A. R. Boyd, and J. S. Aitchison, *Phys. Rev. Lett.* **81**, 3383 (1998).
- [5] R. Morandotti, H. S. Eisenberg, Y. Silberberg, M. Sorel, and J. S. Aitchison, *Phys. Rev. Lett.* **86**, 3296 (2001).
- [6] J. W. Fleischer, T. Carmon, M. Segev, N. K. Efremidis, and D. N. Christodoulides, *Phys. Rev. Lett.* **90**, 023902 (2003).
- [7] D. N. Christodoulides and R. I. Joseph, *Opt. Lett.* **13**, 794 (1988).
- [8] H. G. Winful, *Appl. Phys. Lett.* **46**, 527 (1985).
- [9] N. K. Efremidis and D. N. Christodoulides, *Phys. Rev. A* **67**, 063608 (2003).
- [10] S. Theodorakis and E. Leontidis, *J. Phys. A* **30**, 4835 (1997).
- [11] W. O. Li and A. Smerzi, *Phys. Rev. E* **70**, 016605 (2004).
- [12] B. T. Seaman, L. D. Carr, and M. J. Holland, *Phys. Rev. A* **71**, 033622 (2005).
- [13] A. A. Sukhorukov and Y. S. Kivshar, *Phys. Rev. E* **65**, 036609 (2002).
- [14] A. A. Sukhorukov and Y. S. Kivshar, *Phys. Rev. Lett.* **87**, 083901 (2001).
- [15] I. M. Merhasin, B. V. Gisin, R. Driben, and B. A. Malomed, *Phys. Rev. E* **71**, 016613 (2005).
- [16] C. K. R. T Jones, T. Kupper, and K. Schaffner, *ZAMP* **52**, 859 (2001).
- [17] R. K. Jackson and M. I. Weinstein, *J. Stat. Phys.* **116**, 881 (2004).
- [18] J. Leon, *Phys. Rev. E* **70**, 056604 (2004).
- [19] St. Wiggins, *Introduction to Applied Nonlinear Dynamical Systems and Chaos* (Springer-Verlag, Berlin, 1990).
- [20] R. de L. Kronig and W. G. Penney, *Proc. R. Soc. London*

- A130**, 499 (1931); C. Kittel, *Introduction to Solid State Physics* (Wiley, New York, 1976).
- [21] P. J. Y. Louis, E. A. Ostrovskaya, C. M. Savage, and Y. S. Kivshar, Phys. Rev. A **67**, 013602 (2003).
- [22] D. E. Pelinovsky, A. A. Sukhorukov, and Y. S. Kivshar, Phys. Rev. E **70**, 036618 (2004).
- [23] J. Yang and Z. Chen, Phys. Rev. E **73**, 026609 (2006).
- [24] Y. S. Kivshar, D. E. Pelinovsky, T. Cretegny, and M. Peyrard, Phys. Rev. Lett. **80**, 5032 (1998).
- [25] N. Akhmediev, A. Ankiewicz, and R. Grimshaw, Phys. Rev. E **59**, 6088 (1999).
- [26] A. Ankiewicz and N. Akhmediev, IEE Proc.-J: Optoelectron. **150**, 519 (2003).